

Optimal quantum kernels for small data classification

Elham Torabian and Roman V. Krems

*Department of Chemistry, University of British Columbia, Vancouver, B.C. V6T 1Z1, Canada
Stewart Blusson Quantum Matter Institute, Vancouver, B.C. V6T 1Z4, Canada*

(Dated: March 29, 2022)

While quantum machine learning (ML) has been proposed to be one of the most promising applications of quantum computing, how to build quantum ML models that outperform classical ML remains a major open question. Here, we demonstrate an algorithm for constructing quantum kernels for support vector machines that adapts quantum gate sequences to data. The algorithm includes three essential ingredients: greedy search in the space of quantum circuits, Bayesian information criterion as circuit selection metric and Bayesian optimization of the parameters of the optimal quantum circuit identified. The performance of the resulting quantum models for classification problems with a small number of training points significantly exceeds that of optimized classical models with conventional kernels. In addition, we illustrate the possibility of mapping quantum circuits onto molecular fingerprints and show that performant quantum kernels can be isolated in the resulting chemical space. This suggests that methods developed for optimization and interpolation of molecular properties across chemical spaces can be used for building quantum circuits for quantum machine learning with enhanced performance.

Quantum machine learning (QML) has recently emerged as a new research field aiming to take advantage of quantum computing for machine learning (ML) tasks. It has been shown that embedding data into gate-based quantum circuits can be used to produce kernels for ML models by quantum measurements [1–16]. A major question that remains open is whether quantum kernels thus produced can outperform classical kernels for practical ML applications. The advantage of quantum kernels may manifest itself in reducing the computational hardness for big data problems. For example, it has been shown that a classification problem based on the discrete logarithm problem, which is believed to be in the bounded-error quantum polynomial (BQP) complexity class, can be efficiently solved with quantum kernels [17]. However, it is not yet clear if classical big data problems of practical importance can benefit from QML.

The opposite limit is relevant for applications, where observations are exceedingly expensive. For such applications, learning is based on small data. If quantum kernels can produce models with better inference accuracy for small data problems than classical kernels, QML may offer a practical application of quantum computing to classification, interpolation and optimization of functions that are exceedingly expensive to evaluate. However, the generalization performance of quantum kernels is sensitive to the quantum circuit ansatz [1, 18–20]. The choice of the ansatz is an open problem in QML. For variational quantum optimization and quantum simulation applications, a common strategy is to choose a fixed ansatz and optimize the parameters of the quantum circuit [21–33]. However, for most optimal ML models it is necessary to develop algorithms that adapt the ansatz to data. Previous work has addressed this problem by optimizing gate sequences using quantum combs [34] for cloning, storage retrieving, discrimination, estimation, and tomographic characterization of quantum circuits, graph theory [35] to develop quantum Fourier transforms and reversible

benchmarks, quantum triple annealing minimization [36] for quantum annealing applications, reinforcement learning [37] to solve the Max-Cut problem, a variable structure approach [38] for the variational quantum eigensolver for condensed matter and quantum chemistry applications, and multi-objective genetic algorithms [39] for quantum classification models.

In the present work, we demonstrate a general approach for building an optimal ansatz for quantum support vector machines (SVM). SVM is a kernel method that can be used for both classification and regression problems [40]. SVM kernels allow classification of data that are not linearly separable. As a kernel method, SVM is well suited for small data problems. The quantum analog of SVM uses quantum kernels. Here, we show that the performance of quantum SVM can be systematically enhanced by building quantum kernels in a data-adaptable approach. In order to achieve this, we convert the output of the SVM classifier to probabilistic predictions and compute the Bayesian information criterion (BIC) [41, 43]. We develop an algorithm that builds an optimal quantum circuit for a given data set. The algorithm involves two stages: (i) incremental construction of the quantum circuit using BIC as the circuit selection metric; (ii) Bayesian optimization of the resulting circuit parameters. Using two unrelated classification problems, we show that quantum kernels thus obtained outperform standard classical kernels and achieve enhanced inference accuracy for small data problems. The method proposed here is inspired by the work of Duvenaud *et al.* [42] that demonstrated the possibility of enhancing the performance of classical Gaussian process models through compositional kernel search guided by BIC.

Supervised learning for classification uses N input-output pairs $\{\mathbf{x}, y\}$, with inputs \mathbf{x} represented by multi-dimensional vectors and outputs y encoding the class labels. We consider binary classification problems with $y = \{0, 1\}$. For a QML algorithm, the input vectors \mathbf{x}

must be encoded into quantum states. Here, we use the following encoding of n -dimensional vectors $\mathbf{x} \in \mathbb{R}^n$ into states of n qubits, each initially in state $|0\rangle$:

$$|\Phi(\mathbf{x})\rangle = \exp\left(i \sum_k x_k Z_k\right) H^{\otimes n} |0\rangle^{\otimes n} \quad (1)$$

where x_k is the k -th component of vector \mathbf{x} , Z_k is the Pauli Z -gate acting on k -th qubit, and H represents the Hadamard gate putting qubits into coherent superpositions. The state $|\Phi(\mathbf{x})\rangle$ is operated on by a sequence of one- and two-qubit gates to produce a general quantum state $\mathcal{U}|\Phi(\mathbf{x})\rangle$. The measurable quantities

$$k(\mathbf{x}, \mathbf{x}') = |\langle \Phi(\mathbf{x}') | \mathcal{U}^\dagger \mathcal{U} | \Phi(\mathbf{x}) \rangle|^2 \quad (2)$$

have the properties of the kernel of a reproducing kernel Hilbert space and can thus be used as kernels of SVM.

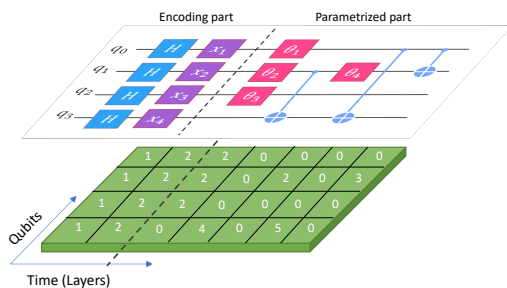


FIG. 1: Schematic diagram of a quantum circuit (upper) used for quantum kernels of SVM and a matrix descriptor (lower) of the gate sequence. Each gate is assigned a numerical descriptor, encoding the type of gate and the index of qubits entangled for CNOT gates shown by blue crosses in the upper diagram.

Here, we propose and demonstrate an algorithm that systematically increases the complexity of \mathcal{U} to enhance the performance of quantum kernels (2). As depicted in Figure 1, we chose \mathcal{U} to consist of L layers, each consisting of one-qubit R_Z gates and/or two-qubit CNOT gates. Each of the R_Z gates for qubit k is parametrized by θ as follows:

$$R_{Z,k}(\theta) = \begin{pmatrix} e^{-i\theta x_k} & 0 \\ 0 & e^{i\theta x_k} \end{pmatrix}. \quad (3)$$

This yields a quantum circuit with the number of free parameters θ equal to the number of R_Z gates. As illustrated in Figure 1 (lower part), for each qubit in each layer, we assign a numerical descriptor that corresponds to a ‘no gate’, CNOT or R_Z . The descriptor of CNOT encodes both of the qubits affected. The numerical descriptors thus generated form a total of $495 + (20 \times 70) \times L$ quantum circuits. We use a strategy equivalent to greedy search to grow the layers of the circuit.

The architecture of the circuit is built incrementally, starting with all possible circuits with only one layer

$L = 1$ after the encoding gates. Using the model selection metric described below, we identify M best kernels with $L = 1$. These circuits are appended by all possible combinations of gates for layer two. The algorithm then selects M best kernels with $L = 2$ and the process is iterated. This greedy search strategy directs the algorithm to increase the complexity of quantum circuits, while improving the performance of quantum kernels. The present results are obtained with $M = 20$. The pseudocode for this algorithm is presented in the supplemental material [55].

Critical to this method is the model selection metric. We convert the output of SVM with quantum kernels to probabilistic predictions and show that Bayesian information criterion (BIC) computed from the resulting probabilities can serve as a metric for selecting quantum circuits in this greedy search algorithm. BIC is defined as follows [41]

$$\text{BIC} = -2 \log \hat{\mathcal{L}} + P \log N \quad (4)$$

where P is the number of free parameters in the quantum kernel equal to the number of R_Z gates and $\hat{\mathcal{L}}$ is the maximized value of likelihood. For the binary classification problem with $y = \{0, 1\}$, we compute $\log \hat{\mathcal{L}}$ as

$$\log \hat{\mathcal{L}} = - \sum_{i=1} [y_i \log(p_i) + (1 - y_i) \log(1 - p_i)], \quad (5)$$

where p_i is the probability of observing class with label $y_i = 1$, obtained from SVM results as described in Ref. [44]. In the current implementation, SVM is trained by maximizing Lagrange dual with a training set [40], while $\log \hat{\mathcal{L}}$ used in Eq. (4) is computed over a separate validation set.

To illustrate the performance of the algorithm proposed here, we use two independent four (4D) and three (3D) dimensional classification problems. For the first example, we use the data from Ref. [45] to classify halide perovskites, with the chemical formula $A_2BB'X_6$ into metals or non-metals. The four components of \mathbf{x} correspond to the ionic radii of the four atoms A, B, B' and X . The second example is a 3D synthetic data set implemented in the Qiskit ML module [46]. Hereafter, we will refer to the two data sets as the perovskite dataset and the *ad hoc* dataset, respectively. We split each data set into 100 random training samples, a validation set with 100 random samples and a test set with 1442 and 4100 samples for the perovskite and *ad hoc* datasets, respectively. The training set is used to train the SVM model with a given quantum kernel, the validation set is used to select quantum circuits, while the test set is used to illustrate the final model performance.

Quantum kernel selection metric. The performance of classification models such as SVM is generally quantified by test accuracy over a holdout set or equivalent metrics, such as the F score [47]. It is convenient to label the two classes as positive and negative and define the true positive rate (TPR) and the true negative rate (TNR) as the

ratio of correct predictions to the total number of test points for a given class. The test/validation accuracy of the model is defined here as the balanced average of TPR and TNR computed over the test/validation set. An alternative frequently used measure of accuracy is the F score, and specifically $F1$ [47]. Figure 2 uses the perovskite dataset to compare the performance of the quantum models with quantum circuits selected using three different metrics: accuracy, $F1$ score and BIC, all computed over the validation sets. The results demonstrate that the classification accuracy or $F1$ score cannot be used as metrics for quantum circuit selection. On the other hand, BIC leads to both better models for each layer L and significant improvement of the quantum classification models as the kernel complexity increases. We observe a similar trend for the other data set (not shown).

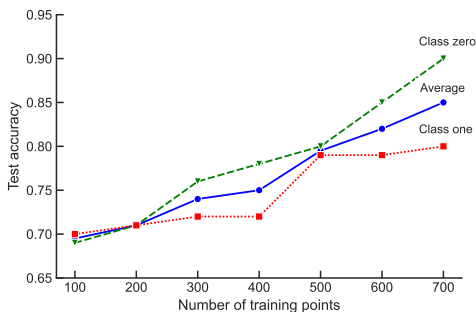
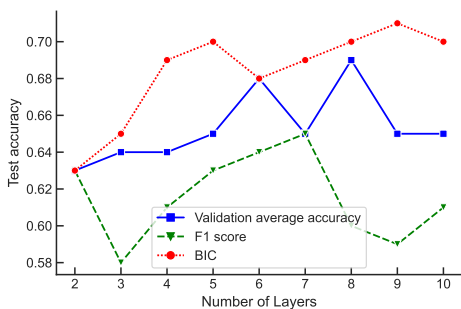


FIG. 2: Upper: Quantum classification model accuracy averaged over two classes over the holdout test set as a function of the number of layers in \mathcal{U} constructed using three model selection metrics: BIC (circles), validation accuracy (squares), $F1$ score (triangles). The models are trained with 100 training points. Lower: Improvement of the quantum classification accuracy with the number of training points. Class-specific test accuracy represents TPR and TNR, as defined in text.

BIC is known to be a rigorous model selection metric asymptotically, in the limit of a large number of training points [40]. For a family of models, each with BIC_m , the probability of model m can be estimated as $e^{-BIC_m/2} / \sum_i e^{-BIC_i/2}$. If the family of K models includes the true model, the probability of the correct model approaches one as $K \rightarrow \infty$ [40]. It is in this limit

that the integral yielding marginal likelihood can be replaced with an expression in terms of the maximized likelihood based on the Laplace approximation, yielding Eq. (4). However, Eq. (4) may not be valid in the small data limit. Our results in Figure 2 show that BIC remains an effective selection metric for quantum models trained with as few as 100 training points. Figure 3 shows the dependence of the lowest value of BIC for both classification problems on the number of layers in the quantum kernels, for models trained with 100 points. The results show that BIC decreases monotonically with the number of layers in the quantum kernels, exhibiting a more significant drop at $L = 1 - 6$.

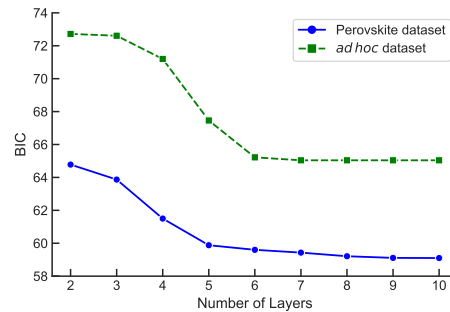


FIG. 3: Bayesian information criterion for the best classification model of a given layer L as a function of the number of layers in \mathcal{U} for quantum models trained with 100 training points.

Classical vs. quantum classification models. Figure 4 compares the results of the predictions of the best quantum models with the classical models based on commonly used optimized kernels. Specifically, we train four classical models with the radial basis function (RBF), linear, cubic polynomial and sigmoid kernel functions. The models are trained with the same number and distribution of training points as for the quantum models and the parameters of each kernel function are optimized to minimize the error over identical validation sets for all models. The quantum models are built using two steps. First, we construct the best quantum kernel for each number of layers L , as described above. The prediction accuracy of SVM models with quantum kernels thus obtained is shown by circles. Second, we vary the parameters θ of all R_Z gates in the best quantum kernel for a given L to minimize error on the validation set. This leads to quantum kernels with both the optimal architecture and optimized gate parameters. The prediction accuracy of SVM models with such kernels is shown in Figure 4 by diamonds. The parameters of the R_Z gates are optimized using Bayesian optimization. The technical details of the optimization procedure are described in SM [55].

For a binary classification problem, one can evaluate the model test accuracy for each class separately. The performance of classification models is generally limited by the lower of the two prediction accuracies. Figure 4

shows the lowest test accuracy of the best models trained with $N = 100$. It can be seen that the performance of quantum models significantly exceeds the prediction accuracy achievable with classical kernels considered. SM presents the detailed comparisons of classical and quantum model predictions for each class separately.

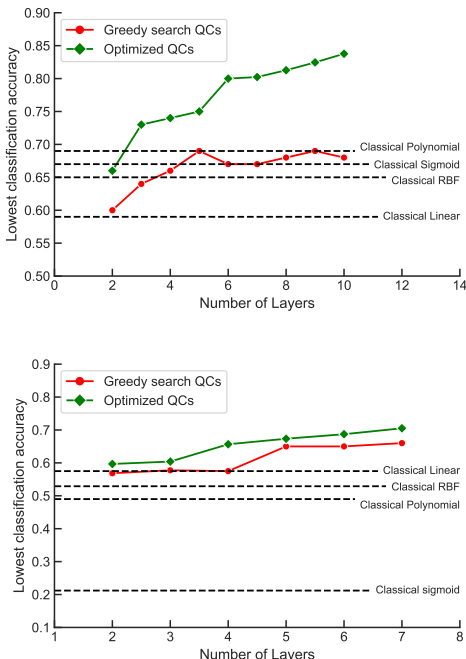


FIG. 4: Lowest prediction accuracy evaluated on the holdout test set for the perovskite (upper) and *ad hoc* (lower) classification problems. The horizontal broken lines show the best accuracy for SVM models with the classical kernels indicated as labels. The classical kernels are optimized using the validation set. The symbols show the results of the best quantum model for each layer L : circles – quantum kernels constructed using greedy search with fixed parameters of all quantum gates; diamonds – best quantum circuit with optimized parameters of R_Z gates.

Molecular fingerprint representation of quantum circuits. It is instructive to examine if there is a qualitative difference between quantum kernels with good performance and quantum kernels that are not suitable for the present classification problems. To separate the two types of kernels, we take advantage of descriptors developed for ML in chemical space. Molecules can be represented by a variety of numerical descriptors developed for drug design, chemoinformatics, computational combinatorial chemistry, and virtual screening applications [48–52]. These descriptors generally account for atom connectivity and the type of atoms [53]. We map quantum circuits onto molecules and use the corresponding molecular fingerprints implemented in Ref. [54]. As illustrated in Figure 5 (upper panel), the mapping is achieved by as-

signing each type of quantum gate a particular atom or atom group, chosen arbitrarily but used consistently, i.e. the same atom must be used for the same type of gate. The specific mapping used here is $R_Z \rightarrow C$, CNOT(1) $\rightarrow O$, CNOT(2) $\rightarrow S$, CNOT(3) $\rightarrow Se$, where the index of CNOT indicates the target qubit. The valency of all atoms is saturated by attaching the hydrogen atoms to produce stable molecules. The 4-qubit circuit is then considered to grow along four branches of an sp^3 -hybridized carbon atom (circled in Figure 5). This generates high-dimensional molecular fingerprints that can be used as detailed descriptors of quantum circuits.

We classify all quantum kernels into ‘good’, defined as kernels that yield better accuracy than the best classical model considered here, and ‘bad’, which correspond to quantum models that underperform the best classical model. Using principle component analysis, we reduce the high-dimensional molecular descriptors to two eigenvectors of the covariance matrix. Figure 5 (lower panel) shows the distribution of quantum kernels in this two dimensional space for the perovskite dataset. We observe a similar result (not shown) for the *ad hoc* data set.

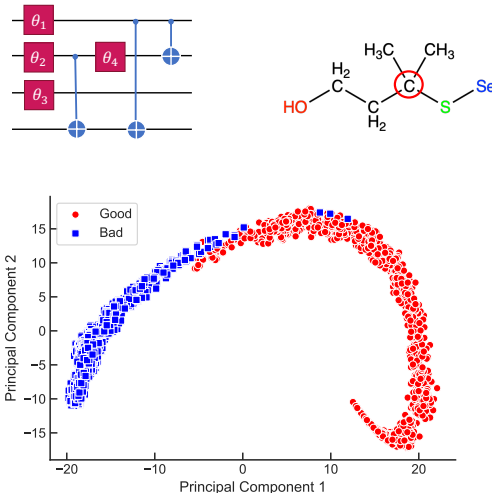


FIG. 5: Upper: Illustration of mapping of a quantum circuit onto a molecule. Lower: Quantum models yielding accuracy below (blue squares) and above (red circles) the performance of the best classical model in the space of two leading eigenvectors of the covariance matrix for molecular fingerprints.

Figure 5 shows that there is a clear separation between quantum kernels, depending on their performance. This indicates that the sequence of gates selected by BIC in the circuit construction algorithm is qualitatively distinct and must have some specific structure that determines the performance of the resulting kernels. We could not identify this structure due to complexity of the quantum circuits obtained. However, Figure 5 suggests that molecular fingerprints can be used as physical descriptors of quantum circuits. This can be exploited to develop

algorithms for optimal quantum kernel construction by interpolation and optimization in chemical spaces.

Conclusion. We have demonstrated an algorithm for constructing optimal quantum kernels for quantum SVM that adapt to data for classification problems. The algorithm includes three essential ingredients: greedy search in the space of quantum circuits, Bayesian information criterion as the circuit selection metric and Bayesian optimization of the parameters of the most optimal quantum kernel architecture identified. Our results show that BIC can select performant quantum kernels, even for problems with a small number of training points, while validation accuracy fails as a quantum kernel selection metric in

this limit. We illustrate the possibility of mapping quantum circuits onto molecular fingerprints. This suggests that methods developed for optimization and prediction of molecular properties across chemical spaces can be used for building quantum circuits with optimized properties for QML. The present work offers a new approach to identify QML models with enhanced performance, potentially making QML useful for practical applications, including interpolation, classification and optimization of objective functions that are exceedingly difficult to evaluate.

This work was supported by NSERC of Canada.

-
- [1] M. Schuld, Quantum machine learning models are kernel methods, *arXiv e-prints*, arXiv:2101 (2021).
- [2] M. Schuld and N. Killoran, Quantum machine learning in feature hilbert spaces, *Phys. Rev. Lett.* **122**, 040504 (2019).
- [3] M. Schuld, Supervised quantum machine learning models are kernel methods, *arXiv preprint arXiv:2101.11020*, (2021).
- [4] P. Rebentrost, M. Mohseni, and S. Lloyd, Quantum support vector machine for big data classification, *Phys. Rev. Lett.* **113**, 130503 (2014).
- [5] V. Havlíček, A. D. Córcoles, K. Temme, A. W. Harrow, A. Kandala, J. M. Chow, and J. M. Gambetta, Supervised learning with quantum-enhanced feature spaces, *Nature* **567**, 209–212 (2019).
- [6] R. Mengoni and A. Di Pierro, Kernel methods in quantum machine learning, *Quantum Mach. Intell.* **1**, 65–71 (2019).
- [7] K. Bartkiewicz, C. Gneiting, A. Černoč, K. Jiráková, K. Lemr, and F. Nori, Experimental kernel-based quantum machine learning in finite feature space, *Sci. Rep.* **10**, 1–9 (2020).
- [8] D. K. Park, C. Blank, and F. Petruccione, The theory of the quantum kernel-based binary classifier, *Phys. Lett. A* **384**, 126422 (2020).
- [9] Y. Suzuki, H. Yano, Q. Gao, S. Uno, T. Tanaka, M. Akiyama, and N. Yamamoto, Analysis and synthesis of feature map for kernel-based quantum classifier, *Quantum Mach. Intell.* **2**, 1–9 (2020).
- [10] J. E. Park, B. Quanz, S. Wood, H. Higgins, and R. Harishankar, Practical application improvement to Quantum SVM: theory to practice, *arXiv preprint arXiv:2012.07725*, (2020).
- [11] R. Chatterjee and T. Yu, Generalized coherent states, reproducing kernels, and quantum support vector machines, *arXiv preprint arXiv:1612.03713*, (2016).
- [12] J. R. Glick, T. P. Gujarati, A. D. Corcoles, Y. Kim, A. Kandala, J. M. Gambetta, and K. Temme, Covariant quantum kernels for data with group structure, *arXiv preprint arXiv:2105.03406*, (2021).
- [13] C. Blank, D. K. Park, J. K. K. Rhee, and F. Petruccione, Quantum classifier with tailored quantum kernel, *Npj Quantum Inf.* **6**, 1–7 (2020).
- [14] S. L. Wu, S. Sun, W. Guan, C. Zhou, J. Chan, C. L. Cheng, T. Pham, Y. Qian, A. Z. Wang, R. Zhang, and M. Livny, Application of quantum machine learning using the quantum kernel algorithm on high energy physics analysis at the LHC, *Phys. Rev. Res.* **3**, 033221 (2021).
- [15] T. Haug, C. N. Self, and M. S. Kim, Large-scale quantum machine learning, *arXiv preprint arXiv:2108.01039*, (2021).
- [16] M. Otten, I. R. Goumiri, B. W. Priest, G. F. Chapline, and M. D. Schneider, Quantum machine learning using gaussian processes with performant quantum kernels, *arXiv preprint arXiv:2004.11280*, (2020).
- [17] Y. Liu, S. Arunachalam, and K. Temme, A rigorous and robust quantum speed-up in supervised machine learning, *Nat. Phys.* **17**, 1013–1017 (2021).
- [18] M. Cerezo, A. Arrasmith, R. Babbush, S. C. Benjamin, S. Endo, K. Fujii, J. R. McClean, K. Mitarai, X. Yuan, L. Cincio, and P. J. Coles, Variational quantum algorithms, *Nat. Rev. Phys.* **3**, 625–644 (2021).
- [19] K. Nakaji, H. Tezuka, and N. Yamamoto, Quantum-enhanced neural networks in the neural tangent kernel framework, *arXiv preprint arXiv:2109.03786*, (2021).
- [20] E. Peters, J. Caldeira, A. Ho, S. Leichenauer, M. Mohseni, H. Neven, P. Spentzouris, D. Strain, and G. N. Perdue, Machine learning of high dimensional data on a noisy quantum processor, *Npj Quantum Inf.* **7**, 1–5 (2021).
- [21] M. Schuld, R. Sweke, and J. J. Meyer, Effect of data encoding on the expressive power of variational quantum-machine-learning models, *Phys. Rev. A* **103**, 032430, (2021).
- [22] K. Mitarai, M. Negoro, M. Kitagawa, and K. Fujii, Quantum circuit learning, *Phys. Rev. A* **98**, 032309, (2018).
- [23] M. Watabe, K. Shiba, M. Sogabe, K. Sakamoto, and T. Sogabe, Quantum circuit parameters learning with gradient descent using backpropagation, *arXiv preprint arXiv:1910.14266*, (2019).
- [24] J. Qi, C. H. H. Yang, and P. Y. Chen, QTN-VQC: An End-to-End Learning framework for Quantum Neural Networks, *arXiv preprint arXiv:2110.03861*, (2021).
- [25] K. Terashi, M. Kaneda, T. Kishimoto, M. Saito, R. Sawada, and J. Tanaka, Event classification with quantum machine learning in high-energy physics, *J. Comput. Softw. Big Sci.* **5**, 1–11, (2021).
- [26] S. Y. C. Chen, C. M. Huang, C. W. Hsing, and Y. J. Kao, Hybrid quantum-classical classifier based on tensor network and variational quantum circuit, *arXiv preprint*

- arXiv:2011.14651*, (2020).
- [27] A. Blance and M. Spannowsky, Quantum machine learning for particle physics using a variational quantum classifier, *J. High Energy Phys.* **2021**, 1–20, (2021).
- [28] Y. Kwak, W. J. Yun, S. Jung, J. K. Kim, and J. Kim, Introduction to quantum reinforcement learning: Theory and pennylane-based implementation, *2021 International Conference on Information and Communication Technology Convergence (ICTC)*, 416–420, (2021).
- [29] D. Sierra-Sosa, J. Arcila-Moreno, B. Garcia-Zapirain, C. Castillo-Olea, and A. Elmaghraby, Dementia prediction applying variational quantum classifier, *arXiv preprint arXiv:2007.08653*, (2020).
- [30] S. Y. C. Chen, C. H. H. Yang, J. Qi, P. Y. Chen, X. Ma, and H. S. Goan, Variational quantum circuits for deep reinforcement learning, *IEEE Access* **8**, 141007–141024, (2020).
- [31] S. Lloyd, M. Schuld, A. Ijaz, J. Izaac, and N. Killoran, Quantum embeddings for machine learning, *arXiv preprint arXiv:2001.03622*, (2020).
- [32] T. Hubregtsen, D. Wierichs, E. Gil-Fuster, P. J. H. Derks, P. K. Faehrmann, and J. J. Meyer, Training quantum embedding kernels on near-term quantum computers, *arXiv preprint arXiv:2105.02276*, (2021).
- [33] L. P. Henry, S. Thabet, C. Dalyac, and L. Henriët, Quantum evolution kernel: Machine learning on graphs with programmable arrays of qubits, *Phys. Rev. A* **104**, 032416, (2021).
- [34] G. Chiribella, G. M. D’Ariano, and P. Perinotti, Quantum circuit architecture, *Phys. Rev. Lett.* **101**, 060401 (2008).
- [35] A. Shafaei, M. Saeedi, and M. Pedram, Optimization of quantum circuits for interaction distance in linear nearest neighbor architectures, *In 2013 50th ACM/EDAC/IEEE Design Automation Conference (DAC)*, 1–6 (2013).
- [36] L. Gyongyosi and S. Imre, Quantum circuit design for objective function maximization in gate-model quantum computers, *Quantum Inf. Process.* **18**, 1–33 (2019).
- [37] T. Fösel, M. Y. Niu, F. Marquardt, and L. Li, Quantum circuit optimization with deep reinforcement learning, *arXiv preprint arXiv:2103.07585*, (2021).
- [38] M. Bilkis, M. Cerezo, G. Verdon, P. J. Coles, and L. Cincio, A semi-agnostic ansatz with variable structure for quantum machine learning, *arXiv preprint arXiv:2103.06712* (2021).
- [39] S. Altares-López, A. Ribeiro, and J. J. García-Ripoll, Automatic design of quantum feature maps, *Quantum Sci. Technol.* **6**, 045015 (2021).
- [40] T. Hastie, R. Tibshirani, and J. H. Friedman, The elements of statistical learning: data mining, inference, and prediction, *Springer* **2**, (2009).
- [41] A. A. Neath and J. E. Cavanaugh, The Bayesian information criterion: background, derivation, and applications, *Wiley Interdiscip. Rev. Comput. Stat.* **4**, 199–203, (2012).
- [42] D. K. Duvenaud, J. Lloyd, R. Grosse, J. B. Tenenbaum, and Z. Ghahramani, Structure discovery in nonparametric regression through compositional kernel search, *Proceedings of the 30th International Conference on Machine Learning Research* **28**, 1166 (2013).
- [43] B. Shahriari, K. Swersky, Z. Wang, R. P. Adams, and N. De Freitas, Taking the human out of the loop: A review of Bayesian optimization, *Proc. IEEE* **104**, 148–175 (2015).
- [44] T. F. Wu, C. J. Lin, and R. Weng, Probability estimates for multi-class classification by pairwise coupling, *Adv. Neural Inf. Process. Syst.* **16**, (2003).
- [45] A. Jain, S. P. Ong, G. Hautier, W. Chen, W. D. Richards, S. Dacek, S. Cholia, D. Gunter, D. Skinner, G. Ceder, and K. A. Persson, The Materials Project: A materials genome approach to accelerating materials innovation, *APL Mater.* **1**, 011002 (2013).
- [46] Qiskit Machine Learning Development Team, Qiskit machine learning, <https://qiskit.org/documentation/machine-learning> (2021).
- [47] T. Fawcett, An introduction to ROC analysis, *Pattern Recognit. Lett.* **27**, 861–874 (2006).
- [48] A. U. Khan, Descriptors and their selection methods in QSAR analysis: paradigm for drug design, *Drug Discov. Today* **21**, 1291–1302 (2016).
- [49] V. Kamath and A. Pai, Application of Molecular Descriptors in Modern Computational Drug Design—An Overview, *Res. J. Pharm. Technol.* **10**, 3237–3241 (2017).
- [50] L. Xue and J. Bajorath, Molecular descriptors in chemoinformatics, computational combinatorial chemistry, and virtual screening, *Comb. Chem. High Throughput Screen.* **3**, 363–372 (2000).
- [51] J. M. Amigó, J. Gálvez, and V. M. Villar, A review on molecular topology: applying graph theory to drug discovery and design, *Naturwissenschaften* **96**, (2009).
- [52] R. Todeschini and V. Consonni, Handbook of molecular descriptors, *John Wiley & Sons*, (2008).
- [53] M. Seo, H. K. Shin, Y. Myung, S. Hwang, and K. T. No, Development of Natural Compound Molecular Fingerprint (NC-MFP) with the Dictionary of Natural Products (DNP) for natural product-based drug development, *J. Cheminformatics* **12**, 1–17 (2020).
- [54] G. Landrum, RDKit: Open-Source Cheminformatics Software, <http://www.rdkit.org/>.
- [55] Supplemental Material

Supplemental Material for Optimal quantum kernels for small data classification

Elham Torabian and Roman V. Krems¹

¹*Department of Chemistry, University of British Columbia, Vancouver, B.C. V6T 1Z1, Canada
Stewart Blusson Quantum Matter Institute, Vancouver, B.C. V6T 1Z4, Canada*

(Dated: March 29, 2022)

The following is the pseudocode for the algorithm of this work:

Algorithm 1 Quantum kernel optimization for SVM

Input:

- (i) Classification data set $\{\mathbf{x}, y\}$: including training, validation and test sets;
- (ii) A set of quantum gates;
- (iii) L_{\max} : number of quantum circuit (QC) layers;
- (iv) M : number of QC for local search;
- (v) \mathcal{N} : maximum number of iterations in Bayesian optimization (BO).

Output: An optimal QC architecture and optimal gate parameters θ^*

```
1: Build a QC that encodes inputs into gate parameters
2: Initialize list OptimalQC with  $M$  identical QC
3: for All  $1 < L \leq L_{\max}$  do
4:   for Each element in OptimalQC do
5:     for All possible gate combinations in layer  $L$  do
6:       Append a layer of gates to QC
7:       Compute the quantum kernel  $k(\mathbf{x}, \mathbf{x}')$ 
8:       Train an SVM model with  $k(\mathbf{x}, \mathbf{x}')$ 
9:       Convert outputs of SVM to probabilistic predictions
10:      Calculate BIC with the validation set
11:    end for
12:  end for
13:  Sort all resulting quantum kernels by BIC in increasing order
14:  Replace list OptimalQC with  $M$  lowest BIC entries
15: end for
16: for QC circuit with lowest BIC  $\in$  OptimalQC do
17:   while iteration  $\leq \mathcal{N}$  do
18:     Determine the gate parameters  $\theta$  using the acquisition function of BO
19:   end while
20:   Assign the resulting gate parameters to  $\theta^*$ 
21: end for
```

BAYESIAN OPTIMIZATION (BO)

BO is a gradient-free optimization approach that can be used for finding the global maximizer (or minimizer) of a non-convex black-box function (unknown objective function f) [1]. We apply BO to optimize the parameters of the quantum circuit θ . The objective function for this optimization is BIC = $f(\theta)$ computed with the validation set. BO is initialized by evaluations of BIC at 50 randomly selected combinations of parameters θ . A Gaussian process (GP) model $\mathcal{F}(\theta)$ is trained using the results of these evaluations. Each GP model \mathcal{F} is characterized by the mean $\mu(\theta)$ and the uncertainty $\sigma(\theta)$, which are functions of θ . The subsequent evaluations of BIC are performed at the maximum of the acquisition function $\alpha(\theta)$ defined as

$$\alpha(\theta) = \mu(\theta) + \kappa\sigma(\theta) \quad (1)$$

where κ is a hyperparameter that determines the balance between exploration and exploitation. At each iteration, we add the result of new evaluation to the previous sample of θ and re-train the new GP model. The value of κ in Eq. (1) is chosen to be $\kappa = 1$. We use RBF kernels for the GP models \mathcal{F} and run BO for $\sim 10 \times d$ iterations sampling $d \in 2, \dots, 16$ dimensions of the θ parameter space to identify the optimal parameters θ^* .

CLASS-SPECIFIC TEST ACCURACY

For binary classification, one can characterize model accuracy by true positive rate (TPR), true negative rate (TNR) and by the test accuracy defined in the present work as $(\text{TPR} + \text{TNR})/2$. TPR is defined as the ratio of correct predictions to total number of test points for class zero. TNR is defined in the same way for class one. We refer to TPR as test accuracy for class one and TNR as test accuracy for class zero. The main text presents the results for the class, for which the models are least accurate. For completeness, we present here the average test accuracy (Figure SM1) and the test accuracy for each class separately, for two classification problems (Figures SM2 and SM3).

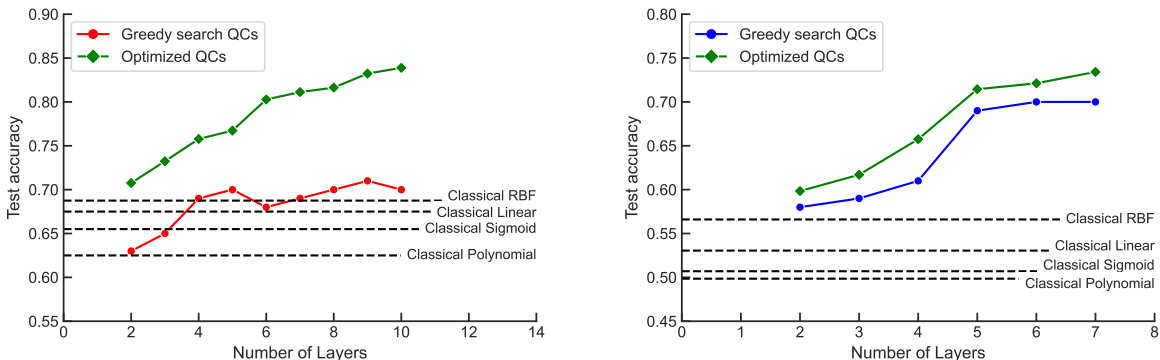


FIG. SM1: Test accuracy evaluated on the holdout test set for the perovskite (left) and *ad hoc* (right) classification problems. The horizontal broken lines show the best accuracy for SVM models with the classical kernels indicated as labels. The classical kernels are optimized using the validation set. The symbols show the results of the best quantum model for each layer L : circles – quantum kernels constructed using greedy search as described in main text with fixed parameters of all quantum gates; diamonds – best quantum circuit with optimized parameters of single-qubit R_Z gates.

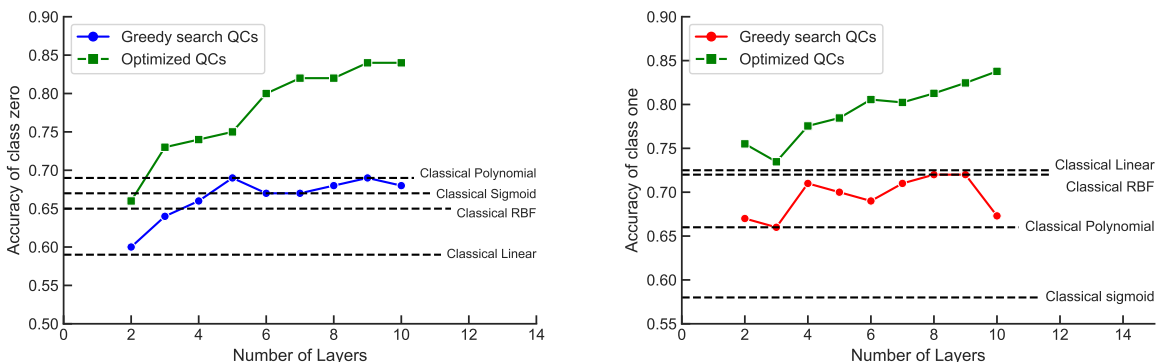


FIG. SM2: Test accuracy of the perovskite classification problem for the class zero (left) and class one (right) sets. The horizontal dashed lines show the best accuracy for SVM models with the classical kernels indicated as labels that they are optimized using the validation set. The symbols show the results of the best quantum model for each layer L : circles – quantum kernels constructed using greedy search as described in main text with fixed parameters of all quantum gates; diamonds – best quantum circuit with optimized parameters of single-qubit R_Z gates.

To validate the perovskite dataset result, the proposed algorithm has been applied for classifying the *ad hoc* dataset- the second dataset- and figure SM3 shows the same trend of increasing the prediction accuracy by increasing the number of layers.

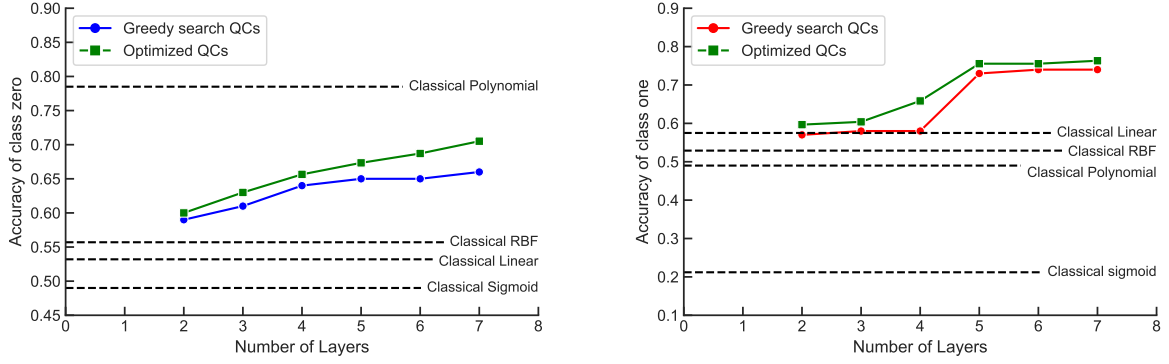


FIG. SM3: Test accuracy of the *ad hoc* classification problem for the class zero (left) and class one (right) sets. The horizontal dashed lines show the best accuracy for SVM models with the classical kernels indicated as labels that they are optimized using the validation set. The symbols show the results of the best quantum model for each layer L : circles – quantum kernels constructed using greedy search as described in main text with fixed parameters of all quantum gates; diamonds – best quantum circuit with optimized parameters of single-qubit R_Z gates.

-
- [1] B. Shahriari, K. Swersky, Z. Wang, R. P. Adams, and N. De Freitas, Taking the human out of the loop: A review of Bayesian optimization, *Proc. IEEE* **104**, 148–175 (2015).